TABLE I. Experimental results.

| $t_0$ (hours) | $C_S{}^{t_0}$ (coinc/min) | $C_S{}^{t_0+12}$ (coinc/min) | $C_s{}^{t_0}$ (coinc/min) | $C_s{}^{t_0+12}$ (coinc/min) | $C_{S+s}{}^{t_0}$ (coinc/min) | $C_{S+s}{}^{t_0+12}$ (coinc/min) | $R_S(t_0)$ | $R_s(t_0)$ | $R_{S+s}(t_0)$ | $H^{t_0}$ (mm Hg) | $H^{t_0+12}$ (mm Hg) |
|---|---|---|---|---|---|---|---|---|---|---|---|
| 0 | 3.002 ±0.029 | 3.074 ±0.031 | 0.0632 ±0.0047 | 0.0547 ±0.0042 | 0.0152 ±0.0021 | 0.0081 ±0.0016 | 0.976 ±0.014 | 1.16 ±0.12 | 1.88 ±0.46 | 508 | 507 |
| 2 | 3.015 ±0.029 | 3.006 ±0.037 | 0.0620 ±0.0041 | 0.0750 ±0.0058 | 0.0152 ±0.0020 | 0.0087 ±0.0020 | 1.002 ±0.016 | 0.83 ±0.09 | 1.75 ±0.47 | 507 | 508 |
| 4 | 3.102 ±0.044 | 3.025 ±0.038 | 0.0545 ±0.0059 | 0.0572 ±0.0052 | 0.0171 ±0.0033 | 0.0076 ±0.0019 | 1.025 ±0.015 | 0.95 ±0.13 | 2.24 ±0.70 | 508 | 508 |
| 6 | 3.051 ±0.039 | 2.994 ±0.035 | 0.0543 ±0.0052 | 0.0577 ±0.0048 | 0.0152 ±0.0027 | 0.0089 ±0.0019 | 1.019 ±0.018 | 0.94 ±0.12 | 1.70 ±0.47 | 509 | 507 |
| 8 | 3.055 ±0.038 | 3.004 ±0.027 | 0.0569 ±0.0051 | 0.0610 ±0.0039 | 0.0139 ±0.0025 | 0.0105 ±0.0016 | 1.016 ±0.015 | 0.93 ±0.10 | 1.32 ±0.31 | 509 | 507 |
| 10 | 3.113 ±0.026 | 2.999 ±0.032 | 0.0542 ±0.0050 | 0.0609 ±0.0056 | 0.0099 ±0.0021 | 0.0122 ±0.0018 | 1.038 ±0.014 | 0.89 ±0.13 | 0.81 ±0.21 | 508 | 507 |

The experimental arrangement for detecting the showers consisted of 3 sets, $ABC$, of Geiger counters placed in a horizontal plane at the vertices of an equilateral triangle of side 6 m: each set had an area $S=8\times10^{-2}$ m². In addition, 3 sets, $DEF$, of counters are placed one above the other near the center of the triangle $ABC$; set $D$ was of ordinary Geiger counters, while sets $E$ and $F$ were of low efficiency counters, (efficiency $r=3$ percent). The area of each set $DEF$ was $s=10^{-2}$ m².

Above the counters there was only the roof of the laboratory, of thickness 1.4 g/cm² of light material, and we have neglected correcting any errors resulting from this.

We recorded simultaneously threefold coincidences between the sets $ABC(C_S)$, threefold coincidences $DEF(C_s)$, and sixfold coincidences $ABC+DEF(C_{S+s})$.

In order to analyze the experimental results, from the point of view of diurnal variations, we divided into two groups the three types of coincidences, the threefolds $C_S$ and $C_s$ and the sixfolds $C_{S+s}$. The first group contained the events recorded between the hours $t_0$ and $(t_0+12)$, (middle European time), and the second, those recorded between $(t_0+12)$ and $(t_0+24)$. We use $C_S{}^{t_0}$, $C_s{}^{t_0}$ and $C_{S+s}{}^{t_0}$ to refer to events of the first group, and $C_S{}^{t_0+12}$, $C_{S+s}{}^{t_0+12}$ to events of the second, and we have calculated the experimental ratios

$$C_S{}^{t_0}/C_S{}^{t_0+12}=R_S(t_0),\quad C_s{}^{t_0}/C_s{}^{t_0+12}=R_s(t_0),$$
$$C_{S+s}{}^{t_0}/C_{S+s}{}^{t_0+12}=R_{S+s}(t_0).$$

In Table I we give the experimental results, including also in column 8 the weighted mean values of the atmospheric pressure. It will be seen from this table that, while $R_S(t_0)$ and $R_s(t_0)$ remain constant at a value near unity, within the experimental errors, $R_{S+s}(t_0)$ is greater than unity for $t_0$ between 0 and 8 hours, and less than unity for $t_0$ greater than 8 hours.

This rather large variation of $R_{S+s}$ with $t_0$, is rendered somewhat uncertain by the large statistical errors, but, assuming that it is significant, we can exclude the possibility that it is due to instrumental effects (casual coincidences, interference, etc.) or to barometric effects. Furthermore, from a rough evaluation of its magnitude, it seems that an effect due to the diurnal variation of temperature of the atmosphere would produce, if at all, a variation of $R_{S+s}$ opposite to that observed.

In an endeavor to explain these experimental results, we observe that:

(a) the coincidences $C_S$, as is well known, are caused chiefly by showers of density $\Delta\simeq 1/S=12$ m$^{-2}$;

(b) the coincidences $C_s$ are due chiefly[2] to heavily ionizing particles, to groups of particles locally associated and to extensive showers of density much greater than 12 m$^{-2}$;[3]

(c) the coincidences $C_{S+s}$ are caused by simultaneous events of type (a) and (b), and chiefly by high density showers,[3] as can be seen from an examination of the function

$$F(\Delta)=K\int_0^{\Delta}(1-\exp[-S\Delta])^3 \times(1+\exp[-s(2r-r^2)\Delta])\cdot\Delta^{-(\gamma+1)}d\Delta, \quad (1)$$

which gives the number of coincidences due to showers of density less than $\Delta$, and is written under the usual hypotheses applicable to arrangement similar to ours.

To explain the results, we make the tentative assumption that the showers of density greater than a certain value $\Delta_1$, have an intensity zero during the 12 hours from 4 P.M. to 4 A.M., during which time, in fact, the ratio $R_{S+s}$ is less than unity. On this hypothesis,

$$F(\infty)/F(\Delta_1)=2.2$$

and using this and Eq. (1) we calculate $\Delta_1\simeq 500$ m$^{-2}$.

Such a density cutoff during 12 hours is perfectly compatible with the values found for $R_S$ since, as has been said, these are due mostly to showers of density less than $\Delta_1$, and even with the values found for $R_S$ as only a small fraction of the coincidences $C_S$ are due to showers of high density.

It is generally assumed that the energy of primaries responsible for showers of mean density $\Delta\simeq 500$ m$^{-2}$ is of the order $10^{16}$ ev. We consider it reasonable to assume that the diurnal effect observed for the showers refers to primaries of energy greater than $10^{16}$ ev.

A similar analysis applied to the results of other experiments,[4,5] carried out at the Laboratorio Della Testa Grigia, gives independent indication of a diurnal variation of the type described above.

We are continuing further experiments in order to examine more closely this effect, and we hope shortly to communicate these additional results, together with a fuller discussion of the problem.

* Now at the Istituto di Fisica del'Università di Pisa.

[1] We were prompted to this analysis by a suggestion of Professor E. Amaldi, after his recent talk about this subject with Professor H. Alfvén.

[2] De Marco, Martelli, and Salvetti, Nuovo Cimento (to be published).

[3] This was confirmed by a cloud chamber which was placed, originally for other purposes, beneath the sets $DEF$.

[4] Amaldi, Castagnoli, Gigli, and Sciuti, Nuovo Cimento **7**, 401 (1950).

[5] G. Martelli and G. Stoppini, to be published.

## Momentum Representation of the Coulomb Scattering Wave Functions*

E. GUTH AND C. J. MULLIN
*University of Notre Dame, Notre Dame, Indiana*
(Received June 14, 1951)

IN a recent paper[1] it was pointed out that a matrix element of the form

$$M=\int\psi_2{}^*V\psi_1 d\mathbf{r} \quad (1)$$

where $\psi_1$ and $\psi_2$ are the coulomb scattering wave functions of the type introduced by Gordon[2] and used extensively by Sommerfeld,[3] often can be evaluated rather easily if $\psi_1$ and $\psi_2$ are expanded in terms of momentum wave functions $\phi_1(\mathbf{k}')$ and $\phi_2(\mathbf{k}'')$. The mo-

mentum wave functions are the fourier amplitudes in the expansions:

$$\psi_1=\int\phi_1(\mathbf{k}')\exp(i\mathbf{k}'\cdot\mathbf{r})d\mathbf{k}';\quad \psi_2^*=\int\phi_2(\mathbf{k}'')\exp(-i\mathbf{k}''\cdot\mathbf{r})d\mathbf{k}''. \quad (2)$$

Expressed in terms of the momentum functions, the matrix element of Eq. (1) is given by

$$M=\int\int d\mathbf{k}'d\mathbf{k}''\phi_1(\mathbf{k}')\phi_2(\mathbf{k}'')M_{\text{Born}}(\mathbf{k}',\mathbf{k}''), \quad (3)$$

where $M_{\text{Born}}(\mathbf{k}',\mathbf{k}'')$ is the value obtained for the matrix element in the Born approximation (expressed in terms of $\mathbf{k}'$ and $\mathbf{k}''$). Because of the properties of the momentum wave functions, a simple evaluation of the integrals occurring in Eq. (3) can be made in many important problems. For example, suppose the coulomb interaction is weak; then $\phi_1(\mathbf{k}')$ and $\phi_2(\mathbf{k}'')$ are "sharply peaked" at $\mathbf{k}'=\mathbf{k}_1$ and $\mathbf{k}''=\mathbf{k}_2$, respectively (where $\mathbf{k}_1$ and $\mathbf{k}_2$ are the asymptotic values of the wave numbers for the particles described by $\psi_1$ and $\psi_2$). Consequently, unless $M_{\text{Born}}(\mathbf{k}',\mathbf{k}'')$ is a very rapidly varying function of $\mathbf{k}'$ or $\mathbf{k}''$, Eq. (3) reduces to

$$M=M_{\text{Born}}(\mathbf{k}_1,\mathbf{k}_2)\int\phi_1(\mathbf{k}')d\mathbf{k}'\int\phi_2(\mathbf{k}'')d\mathbf{k}''$$
$$=M_{\text{Born}}(\mathbf{k}_1,\mathbf{k}_2)\psi_1(0)\psi_2^*(0) \quad (4)$$

where $\psi_1(0)$ and $\psi_2(0)$ are the coulomb scattering wave functions evaluated at the origin. This simple procedure explains the frequent occurrence of coulomb correction factors of the type given by Eq. (4).

To extend the usefulness of this method of evaluating matrix elements, we have derived explicit expressions for the momentum wave functions. These wave functions, which we have been unable to find in the literature, are of considerable interest for various atomic and nuclear problems. $\phi(\mathbf{k}')$ may be obtained directly from $\psi(\mathbf{r})$ by fourier (or laplace) transformation. In coordinate space

$$\psi(\mathbf{r})=\exp(i\mathbf{k}\cdot\mathbf{r})F(-in,1,i\rho), \quad (5)$$

where $F$ is the confluent hypergeometric function, $\rho=kr-\mathbf{k}\cdot\mathbf{r}$, $\mathbf{k}$ is the asymptotic value of the wave number, and $n=zZe^2/\hbar v$. Using a real $k'$, the fourier transformation yields[4]

$$\phi(\mathbf{k}')=-\frac{1}{2\pi^2}\lim_{\epsilon\to 0}\frac{d}{d\epsilon}\left\{\frac{[k'^2+(\epsilon-ik)^2]^{in}}{[\epsilon^2+(\mathbf{k}'-\mathbf{k})^2]^{1+in}}\right\}. \quad (6)$$

The terms which correspond to the incident and scattered waves may be identified readily since an undistorted plane wave and an undistorted scattered wave have the fourier transforms:[5]

$$T\{\exp(i\mathbf{k}\cdot\mathbf{r})\}=\delta(\mathbf{k}-\mathbf{k}')=\frac{1}{\pi^2}\lim_{\epsilon\to 0}\frac{\epsilon}{[\epsilon^2+(\mathbf{k}'-\mathbf{k})^2]^2} \quad (7)$$

$$T\{\exp(ikr)/r\}=1/[2\pi^2(k'^2-k^2)] \quad (8)$$

where $T\{f\}$ means the three dimensional transform of $f$. From (8) it may be seen that the asymptotic representation of the coordinate wave function corresponds to the point $k'=k$ in momentum space. From (6) and (8) it follows that the amplitude of the scattered wave is given by

$$-2nk/(\mathbf{k}'-\mathbf{k})^{2+2in} \quad (9)$$

with $|\mathbf{k}'|=|\mathbf{k}|$. For $|n|\ll 1$, Eq. (6) acquires the form of the Born result previously treated by Dirac.[6]

The relative simplicity of the momentum wave function given by Eq. (6) results from the fact that the confluent hypergeometric function which occurs in the expression for $\psi(\mathbf{r})$ is expressible in terms of a single parabolic coordinate. Thus, the total momentum function may be obtained, by the convolution theorem, from the fourier transforms of a plane wave and a relatively simple function of a single coordinate. The general coulomb wave function, on the other hand, does not have this essentially one-dimensional character and, consequently, its fourier transform[7] is relatively complicated. The simple character of the one-dimensional fourier (or laplace) transforms (in which only one component of the momentum, e.g., the radial component, is used in the transformation) of many types of wave functions has been emphasized by Dirac;[8] independently, one dimensional laplace transforms have been employed extensively by Kallman and Päsler.[9] Simple transforms are obtained whenever the coordinate wave function satisfies a differential equation of the laplace type.

We are applying both one- and three-dimensional momentum representations of the coulomb scattering wave function to a number of atomic and nuclear problems and will report the results in the near future.

* Supported in part by the ONR.

[1] C. J. Mullin and E. Guth, Phys. Rev. **82**, 141 (1951).
[2] W. Gordon, Z. Physik **48**, 180 (1928).
[3] A. Sommerfeld, *Atombau und Spektrallinien* (F. Vieweg und Sohn, Braunschweig, 1939), II band.
[4] Convergence of the integrals may be insured without the explicit use of convergence factors by taking a complex $k'$. The momentum functions obtained by this procedure are valid for all $k'$ in the lower half of the complex plane. This method has been applied to a discussion of one-dimensional problems by P. A. M. Dirac, Proc. Roy. Soc. (London) **160**, 48 (1937).
[5] Dirac adds to (8) a $\delta$-function which automatically selects the principal value.
[6] P. A. M. Dirac, *Quantum Mechanics* (Oxford University Press, London, 1935), second edition, pp. 195–200.
[7] V. Bargmann, Z. Physik **99**, 576 (1936). The three dimensional transform of the radial part of the coulomb wave function is given by M. Levy, Proc. Roy. Soc. (London) **204**, 145 (1950).
[8] P. A. M. Dirac, see reference 4 and Z. Physik **44**, 585 (1927).
[9] H. Kallmann and M. Päsler, Ann. Physik (6) **2**, 292 (1948).

## The Influence of Magnetization on Ultrasonic Attenuation in a Single Crystal of Nickel or Iron-Silicon*

SHELDON LEVY AND ROHN TRUELL
*Metals Research Laboratory, Brown University, Providence, Rhode Island*
(Received June 7, 1951)

IT has been found that in ferromagnetic single crystals there is an interesting connection between measurements of ultrasonic attenuation[1] (frequency range 5 to 50 megacycles) and the values of a constant magnetic field applied at some fixed direction with the ultrasonic beam direction.

With a single crystal of nickel attenuation measurements were made with the ultrasonic beam direction at approximately 12° to the ⟨111⟩ direction of the crystal. The measurements were made with various values of a constant applied magnetic field applied at right angles to the direction of the ultrasonic beam. The values of the applied magnetic field were varied from zero to saturation in steps as indicated in Fig. 1.

The main features seem to be the magnitude of the change, approximately a factor of nine near 50 megacycles, and the fact that at saturation field the ultrasonic attenuation seems to be quite low and independent of frequency in this range of frequencies.

The photograph of the changes in the pulse amplitude as a function of time, or distance in the material, is shown (at 25 megacycles) in Fig. 2, where the bottom trace is that with saturation field and the top trace is that with zero applied magnetic field. The intermediate stages correspond to the steps shown in Fig. 1.

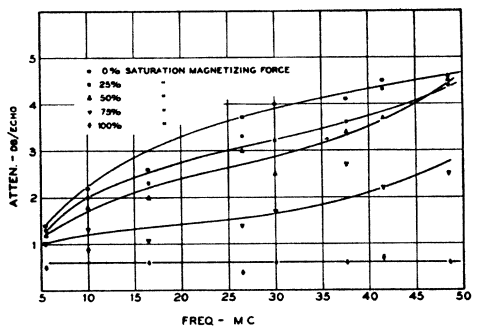


FIG. 1. Attenuation *vs* frequency for nickel at various magnetic field intensities.